



# Form-Finding to Fabrication: A Parametric Shell Structure Fabricated Using an Industrial Robotic Arm with a Hot-Wire End-Effector

Jin-Ho Park<sup>1</sup> · Sejung Jung<sup>1</sup>

Accepted: 24 March 2023 / Published online: 4 April 2023

© The Author(s), under exclusive licence to Springer Nature Switzerland AG 2023, corrected publication 2023

## Abstract

The increasing application of computer technologies in architecture has facilitated interactive collaboration between form-finding and realization. In contrast to conventional methods, various form-finding processes embedded in digital media have recently been investigated. Robotic technologies have also been utilized to execute hazardous tasks and to perform more challenging and complex fabrication in architecture. In this study, we experiment with form-finding and robotic fabrication to explore innovative design possibilities. After selecting a particular site, we determine a rigorous geometric form for construction. Structural analysis of the design is performed to verify the stress distribution and failure mechanisms. The design employs an industrial robotic arm with a hot-wire end-effector to determine an optimum method for full-scale assembly and on-site installation of the design. Finally, this study accurately verifies the constructability of the designed form and evaluated the challenges and opportunities associated with the process. The findings demonstrate that this approach complements the potential impacts of the design process, practice, and aesthetics.

**Keywords** Form-finding · Random circle packing · Parametric shell · Structural stability · Robotic arm fabrication · Assembly

---

✉ Jin-Ho Park  
jinhopark@inha.ac.kr  
Sejung Jung  
s\_w0w@naver.com

<sup>1</sup> Department of Architecture, Inha University, 100 Inharo, Michohol-gu, Incheon 22212, Korea

## Introduction

Contemporary architects are constantly developing complex parametric designs using advanced computer technology. These technologies help improve design capabilities and variabilities and enable the construction of complex geometries with mathematical accuracy. They are also capable of rapidly and directly manufacturing large components based on computer-aided design data. Nonetheless, in practice, the successful implementation of design ideas with a high level of accuracy is often challenging. Recently, industrial robotic arms have demonstrated potential as effective solutions to this problem. Architects have utilized computer media and robotic arms to maximize precision (Weissenböck 2015; McGee and de Leon 2014). Notably, collaborative design and fabrication require new levels of effort, ranging from the design of complex geometries and fabrication techniques using robot control to the use of various end effectors to achieve the required performance (Sharif et al. 2016).

Among other end effectors, robotic hot wire cutting has been widely used with different cutting methods and materials. In particular, Symeonidou et al. (2013) experimented with a straight heated wire to produce ruled surfaces for robotic fabrication for customized concrete formworks. Rust et al. (2016) discussed the spatial wire cutting with curved wire to obtain double-curved, non-ruled surfaces. Jovanovic et al. (2017) tested two robots to perform the cutting process where one holds the EPS material, and the other uses a smaller hotwire tool for cutting the elements. Recently, Yabanigül and Yazar (2021) discussed non-linear robotic hotwire cutting to accurately produce double-curved surfaces with shape memory alloys. An increasing variety of approaches and design experiments using robotic hot wire cutting are being conducted.

Although industrial robotic arms have been widely employed in the past, their use in architecture has been considerably limited compared with similar tasks in different industries. This is because significant challenges must be overcome to facilitate their wide-ranging applications in architecture. The utilization of industrial robotic arms in architecture involves a substantial level of association with other areas, including control and modeling software and different custom-made end effectors for various applications (McGee and de Leon 2014; Reinhardt et al. 2016; Willmann et al. 2018).

This study focuses on exploring a parametric shell design and investigating methods for form-finding and physical prototype fabrication. The following four steps involved in the process from the design to the creation of a physical model were investigated: form finding, structural analysis, robotic fabrication, and assembly. Finally, this study investigated digital-to-fabrication translation processes with regard to the characteristics and limitations of the approaches involved in prototyping parametric shells.

## Form-Finding

The project was conducted in an existing corridor at the Department of Architecture building at Inha University, where a skylight was located. In this setup, although classrooms and design studios are located on both sides of the long corridor, they do not contain aesthetic features (Fig. 1). The corridor appears desolate and lacks

an aesthetic character or a cohesive sense of identity. Intense direct and reflected sunlight occasionally strikes the corridor during the day, and strong glare causes discomfort and strain. In this study, an installation design that prevents the direct reflection of natural light was developed, wherein a secondary structure could be attached to the primary structural system. Although two bays of skylights were present, only one was used for the testbed.

## Development of a Parametric Shell

Part of the corridor was formed with a tall gable-shaped skylight. The second structure within the corridor was integrated into the shape of a skylight. To maximize the height and allow natural light to penetrate the corridor, it was necessary to identify an appropriate design for installation. First, a regular vault design, which is an arched ceiling typically constructed using stones or bricks, was considered. The simple barrel vault is formed by the extrusion of a single circular curve. It is a self-supporting arch that forms a continuous surface tunnel with structural integrity. Different types of ribbed vaults can also be considered depending on their intended function and construction site. In addition to traditional vaults, derivative and atypical designs derived from barrel vault shapes may exist.

### Stage 1: Circle Packing

To experiment with a full-scale parametric shell design, the first stage was to determine the exact geometry of the design while experimenting with various protruding and intruding shapes of the conoid form. Notably, the accurate production of different conoid forms and their contours is challenging. At this stage, the packing degree of the circles within a bounded space was adopted as the initial form-making process. First, a simple algorithm for random circle packing



Fig. 1 Photographs of the plain hallway

was scripted as a generative tool using Grasshopper in Rhinoceros. The basic criteria constituted a setup wherein several circles could be controlled and packed within the top-arched domain of the shell. Careful attention had to be paid to the radii of the circles, which ranged from 500 to 200 mm, considering the actual fabrication of the structure. Then, we created a density image and plugged it into the Grasshopper script, as shown in Fig. 2. The density image serves as a reference for the generation of appropriate circular packing. This script generates random circular packings of varying sizes in a given domain, similar to the density image, such that no overlapping circles are noted. Upon running the algorithm, the packing began immediately. Upon pressing the activation button, scripting continued to change its patterns and eventually terminated at an optimum arrangement. This process assists the generation of a basic circular boundary for shaping conic forms.

## Stage 2: Conoid Shell Form-Finding

Once the basic diagram is determined (Fig. 3a), it is necessary to determine a method for its translation into a three-dimensional (3D) parametric shell. First, the radii of the circular aides at the ends of the conical peaks are determined. Each aide is then randomly allocated to a larger circle. Each aide is composed of two families of circles represented in red and blue (Fig. 3b). One is called a boundary circle for each conoid form, and the other is a conic peak circle inscribed within the boundary circle. For each family, the inner circles indicate peaks with either positive or negative projections. The outer circles form the basic boundaries where the bottom of the conoids is formed. Each center point is then pushed or pulled to varying heights from 200 to 500 mm along the designated directions. By pulling and pushing the surface membrane upward and downward at irregular intervals using circular aides, a simple shell can marginally deform to obtain a structure that differs from a regular shell dome. In other words, each vector of the conic peaks moves in opposite directions. This creates an unusual surface condition resembling a barnacle. Throughout the exercise, in contrast to the geometry of a regular shell, a new parametric shell is formed. The two opposite vectors are neither collinear nor perpendicular to the shell surface at the pushed and pulled points; they are skewed (Fig. 3c). The structure created by the two opposite vectors of tangent forces form a parametric conoid shell.

Once the circular packing pattern was embedded on top of the semi-circular shell, the circular aides were pushed up and pulled down via 3D modeling while considering the boundaries of the neighboring conic surfaces. Thus, a non-uniform shell roof with various uneven conoid forms was obtained. Note that Rhinoceros allows the development of any ruled surface but also facilitates the development of data of a parametric conic form. The peaks of the conoids form a series of holes that serve as diffusers of light in the shape of a funnel. The geometric design of the supporting walls for the lower part of the parametric shell was based on the repetition of a circular pattern. Throughout the design process, a unique parametric shell design based on a semicircular barrel vault was developed. This design was significantly different from that of a conventional vault. The basic parameters and

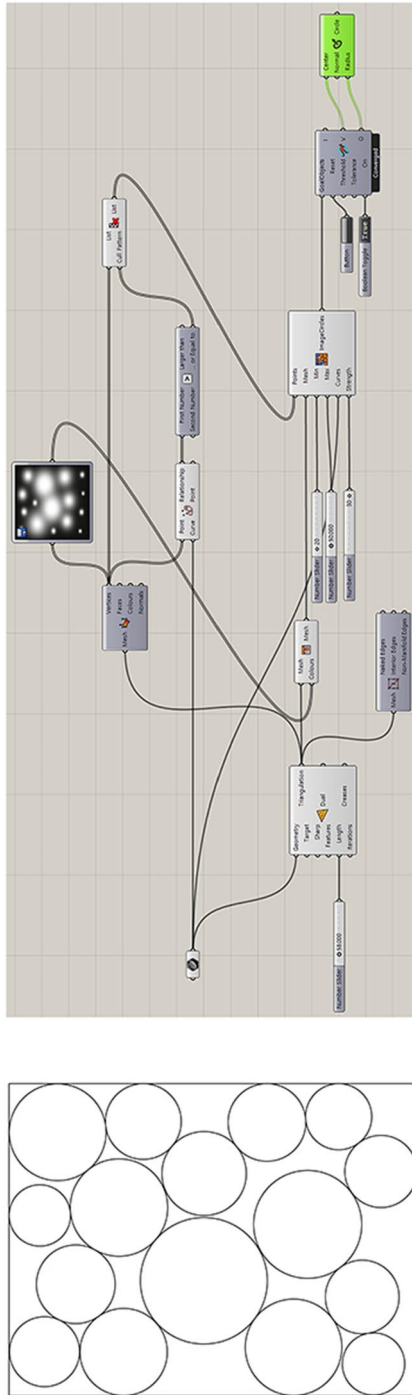
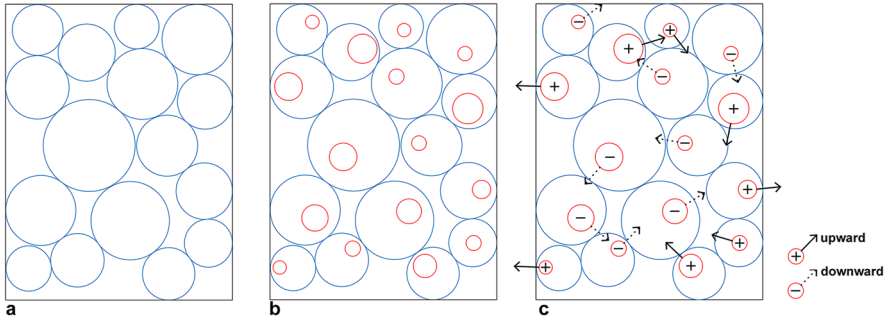


Fig. 2 Random diagram of a circle generated through scripting with Grasshopper in Rhinoceros



**Fig. 3** **a** Basic circle packing pattern; **b** different circular aides at the ends of the shell peaks; **c** two opposite vectors of tangent forces

their distinctive form-finding characteristics are summarized and compared with typical results in Fig. 4.

The foregoing design facilitates the passing of natural light without the apparent presence of an existing skylight. After determining the preliminary design, the amount of sunlight that would enter the corridor through the conoid forms was simulated by adjusting the angles, shapes, and positions of the conoids. Subsequently, areas with effective cumulative sun-exposure conditions during different seasons were simulated to predict the effects of sunlight on the corridor (Fig. 5). With this installation, the corridor was expected to provide a new inspirational atmosphere that would infuse vitality.

## Structural Analysis

For the analysis of structural stability, the MIDAS Gen software was employed, as commonly used and trusted by engineers. The computer model, which was developed from the form-finding in Rhinoceros, had to be exported to the surface model to test structural stability (Fig. 6). The chosen software allowed for the verification of the stress distribution and the formation of failure mechanisms owing to the varying distribution of live loads. In addition, the optimized materials were tested for use in construction. We assumed that the structure could be made of concrete, gypsum, and XPS; therefore, the stress distribution was analyzed for three different materials. The material characteristics are listed in Table 1.

Because the structure was intended to be installed in the interior of a building, we did not consider variable external loads that may induce cracks or deformation. Our analysis revealed that Styrofoam had a weaker compressive strength and lower density than concrete, resulting in lower stress. The tensile strength of each material was set to 10% of each material's compressive strength (Table 2).

The results of the MIDAS Gen analysis, in terms of the maximum principal stresses (expressed in MPa), are presented in Fig. 7. The structural stability of each material was analyzed by exporting the modeling data to MIDAS Gen. The

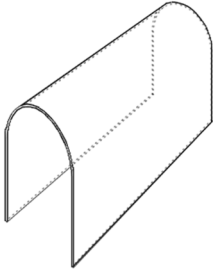
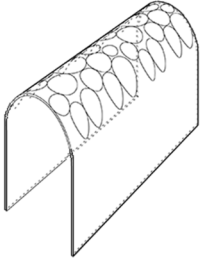

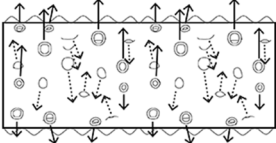
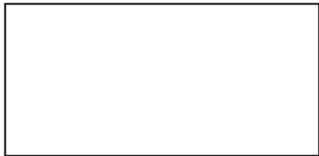
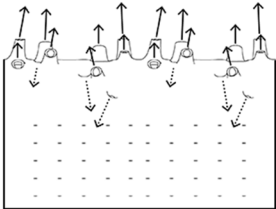
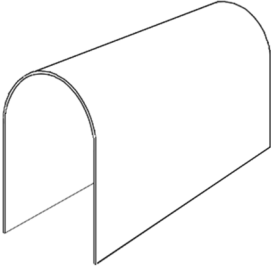
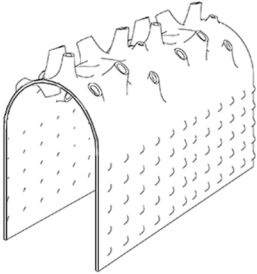
	Barrel vault	Parametric vault
Basic Parameter		
Plan		
Elevation		
Perspective Image		

Fig. 4 Distinctive form-finding characteristics of different shells

results revealed that all the materials had weak tensile strengths; hence, they had to be reinforced when used in the structure. For example, if a structure is fabricated using concrete, a steel rebar should be used to reinforce the structure against potential cracks and deformation. Certain designs can be created efficiently without the need for cumbersome processes; however, this was not the case for the design we developed. It was difficult to realize the compound form of the final design using conventional casting concrete with a wooden mold. It was challenging to mold such a complex design on a small scale (Bechthold 2008; Hawkins et al. 2016). Therefore, Styrofoam was used as an alternative material.

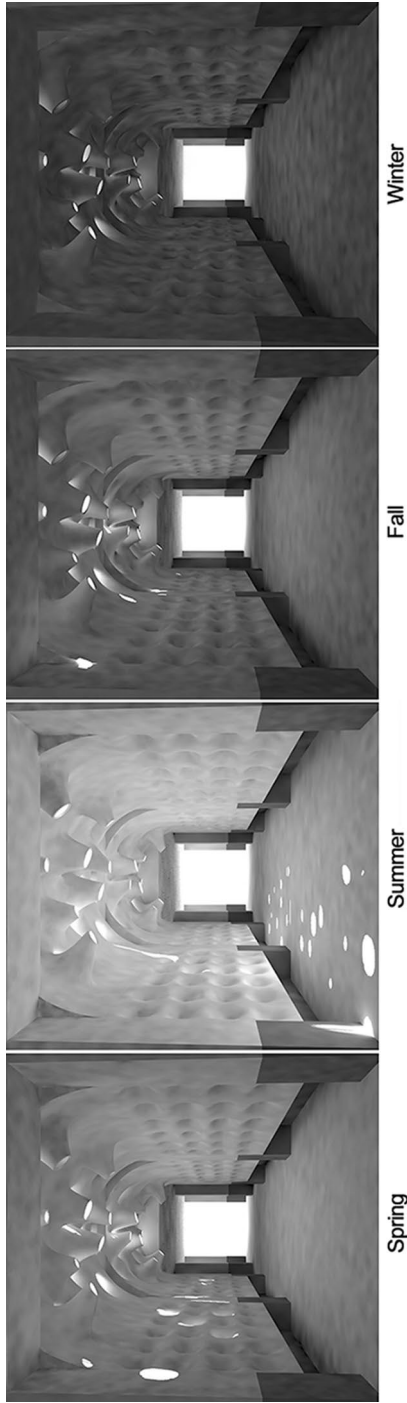
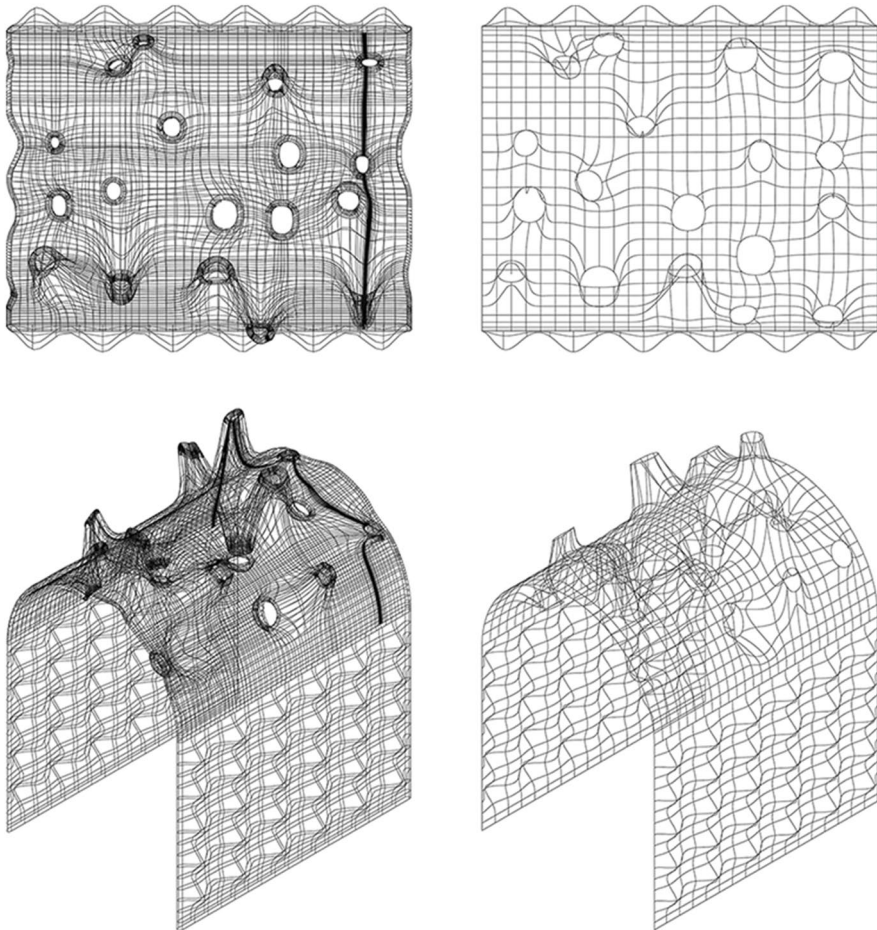


Fig. 5 Simulated spatial effects of natural light during different seasons of the year





**Fig. 6** Solid model of the 0.3 dm file converted into a surface model of a .dwg file

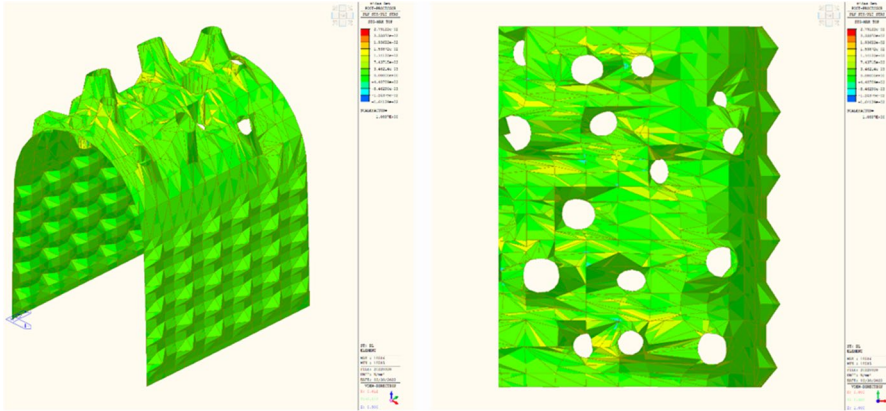
**Table 1** Stress distributions in relation to three materials

	Density (N/mm <sup>3</sup> )	Modulus of elasticity (MPa)	Compressive strength (MPa)	Tensile strength (MPa)
Styrofoam	0.00000015	3.0	0.05	0.005
Concrete	0.00002354	2483.4	21.0	2.1
Gypsum	0.0000087	1740.0	2.4	0.24

Robotic arms enable the efficient on-site fabrication of custom-built structures using Styrofoam, which is typically beyond the capabilities of conventional construction methods. In our study, wire cables with ties were used to reinforce the structure. This reduced the tensile force on the shell structure because the cables

**Table 2** Compressive and tensile strength in relation to three materials

	Styrofoam	Concrete	Gypsum
Maximum compressive strength (MPa)	0.00212	3.45	1.23
Maximum tensile strength (MPa)	0.0204	3.3	1.18



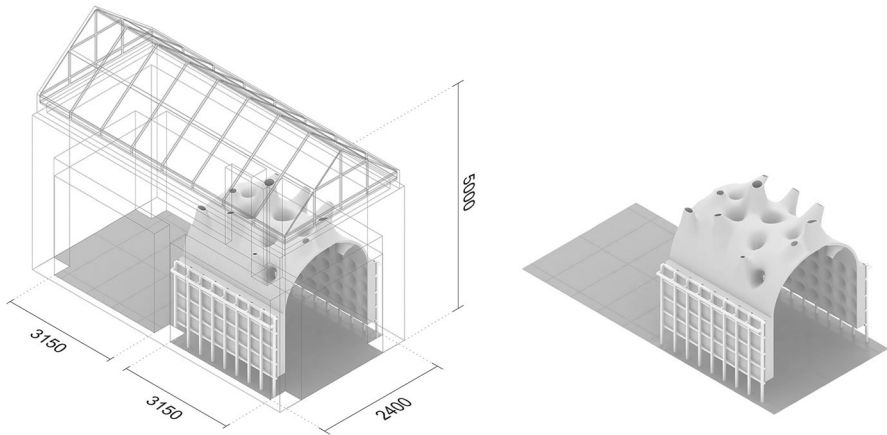
**Fig. 7** Isometric view (a) and top view (b) of the structural analysis performed under the guidance of Prof. Seonghoon Jeong

offered high tensile strength as support. In addition, the design could result in failure unless the sides were anchored to a heavy shell structure; therefore, wooden grid frames were added on both sides of the corridor to anchor the shell structure and provide buttressing strength (Fig. 8).

## Robotic Fabrication Using XPS

One of the most challenging issues in this experiment was the construction of a complex digital design. It could be more efficient to create a design using solid rapid prototyping; however, this process would be costly. Designs realized with surface prototyping using thin skin require additional support. Accordingly, we constructed a structure with a stronger physical medium by using a robotic technique. Experiments on a few key phases are required to translate the design model into a robotic control technique.

In this study, a hot-wire cutter mounted on a robotic arm was used for the custom manufacturing of components. First, we exported the PGF file using a Grasshopper hotwire component and a commercial plugin. Then, it was loaded onto Robotware to move the hotwire cutter along the desired path. Before cutting, the hot-wire cutter must be calibrated to optimize digital simulation and fabrication. After conducting calibration and condition tests, an appropriate method for cutting the components



**Fig. 8** Testing the design with the grid frame on the wall to support the shell structure with and without the skylight frame

with minimal material loss was determined. The digital model was sliced layer-by-layer into components of appropriate sizes that were within the operating range of the hot-wire cutter.

Most industrial robots are effective in performing repetitive and monotonous tasks that are considered highly hazardous to humans or for applications in which manufacturing and assembly are undertaken in hostile environments. Robots are also effective for the automated mass production of components. Moreover, they exhibit significant potential for application in the manufacturing of complex 3D geometrical forms. This is particularly true in a scenario wherein dissimilar components need to be cut and where customized component manufacturing is required. In our design experiment, it was almost infeasible to cut the entire design simultaneously, and construction using other materials such as concrete was challenging. Therefore, the shell structure was subdivided and cut piece-by-piece, and the pieces were subsequently assembled. With the aid of a robot, the time required for assembling the structure decreases, and more systemic construction can be achieved with higher efficiency.

### **Robotic Arm and Hot-Wire Calibration**

A six-axis robotic arm with a payload of 10 kg was deployed for industrial automation to fabricate the shell. A few supplementary tools were required to set up the robotic arm. First, a hot-wire cutter that enabled precise cutting of the ruled surfaces of an expanded polystyrene (EPS) foam was manufactured. A basic frame with a length of 700 mm was developed for the cutter. Subsequently, a nichrome wire with a diameter of 0.6 mm was installed. EPS foam blocks, typically utilized in building construction, were used for the experiment because they could be cut to the sizes required for our project. The tool was calibrated to determine the appropriate

feed rate and heat intensity after establishing a reference axis for the direction of movement of the hot wire. This was performed because an appropriate cutting speed and heat would yield different surface conditions for cutting, resulting in smooth or rippled surfaces. In addition, the kerf width (referring to the parts removed by the cutting process) had to be considered to obtain an accurate output and to reduce the tolerance for defective assemblies. The kerf width increased as the power increased, and the feed rate decreased. If the size of the foam to be cut is large, a considerable amount of power is required to enable the fast movement of the wire cutter. This test requires caution because calibration errors can reduce accuracy. Accordingly, the operator requires time to attain a certain level of manual dexterity to operate the robotic arm by analyzing various cutting parameters and material properties to optimize the cutting process. Through various tests, users must determine the optimal values for the tool and robotic arm through trial and error (Aitchison et al. 2011; Duenser et al. 2020; Park et al. 2021).

## **Ruled Surface and Toolpaths**

Note that each cut generated by the wire is a ruled surface because the cutter is equipped with a taut wire. Each ruled surface is defined by segments that connect the corresponding points of two contours. A series of straight segments constitute the cutting path along which the hot wire cutter moves with ruled surfaces. Accordingly, it was necessary to generate optimal toolpaths for each component and simulate the paths before cutting (Fig. 9). Each component of the model was segmented precisely into three dimensions using Grasshopper in Rhinoceros based on the size of the wire cutter and robotic arm. This process yielded toolpaths that enable the wire cutter to move according to a predefined speed and direction. Toolpaths that play a significant role in obtaining the accurate sizes and shapes of each component must be determined. The intervals between segments are important because excessively long intervals may result in a series of segmented planar surfaces rather than a smooth curved surface. Conversely, if the intervals are excessively short, the hot-wire cutter may move gradually such that the heat-induced foam removal increases. This causes deviations from the anticipated results. Surgically controlled tool paths were simulated using the Grasshopper plug-in. Finally, the components were imported into the robotic arm for cutting.

## **Slicing Components**

The generation of effective data for each component to be cut is one of the most important phases before fabrication. If a problem occurs during the fabrication of parts of the design, the data on the computer can be modified, and fabrication can be resumed immediately after modification. For this process, the appropriate sizes of the smaller components should be determined based on the size capacity of the hot-wire cutter. The shell structure can be sliced into a series of finished components

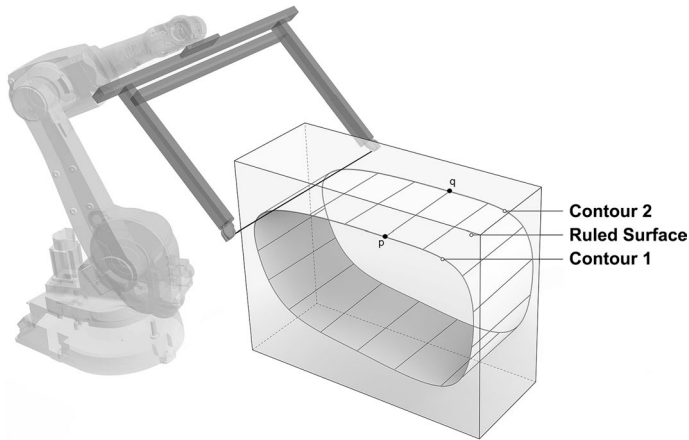


Fig. 9 Tool path in Grasshopper; ruled surface with the intersecting line

that are manufactured using a hot wire. These elements are then assembled on-site by gluing to obtain the final product.

Although the plan footprint for the bay had the following dimensions: 2400 (W)  $\times$  3150 (L), we limited the height of the structure to 3640 (H) mm with an average thickness of 20 mm. It was divided into four sections (Fig. 10). Each section was further subdivided as depicted in Fig. 11. The geometry of the funnel shape at the top (section A) was irregular and complex. Each shape was split into four pieces that fit the size of the hot-wire cutter. The number of pieces in this section was 72. The remaining shell section (Section B) was dissected at 50 mm intervals. The total number of pieces was 63. Each dissected part was further subdivided into five pieces so that the total number of pieces in this section was approximately 315. Section C was simple; therefore, the entire section was split into eight parts (each with a size of 400  $\times$  400 mm) on the left and right sides. The number of components in this section was 16. At the bottom, Section D was repetitively modulated with 400 mm components. The number of components covering both walls was 64. Each component was further subdivided into eight pieces (Fig. 11d) such that the number of pieces to be cut was 512. The total number of pieces to be cut in the design was 915.

Before proceeding with the detailed fabrication, a factory-produced EPS foam was precut into suitable sizes according to the size of the components. This was performed to reduce the disposal and reuse of leftover materials (a large amount of EPS foam was wasted during each cutting). The precut components were categorized into four fundamental types: 450 (W)  $\times$  200 (D)  $\times$  300 (H) mm and 600  $\times$  200  $\times$  750 mm for Section A and 200  $\times$  50  $\times$  750 mm and 265  $\times$  150  $\times$  400 mm for Sections B and C, respectively. Section D measured 50  $\times$  200  $\times$  400 mm. The sizes were determined to efficiently execute the cutting tasks by considering the available range of the cutter mounted on the robotic arm. The more complex the geometry, the higher the material disposal. Hence, it is necessary to estimate the material disposal for each foam block prior to cutting.

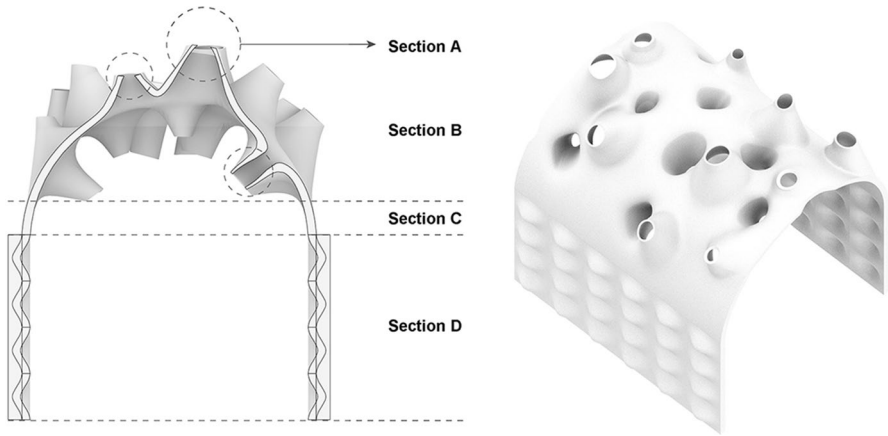


Fig. 10 Subdivision of the design according to the complexity of efficient cutting

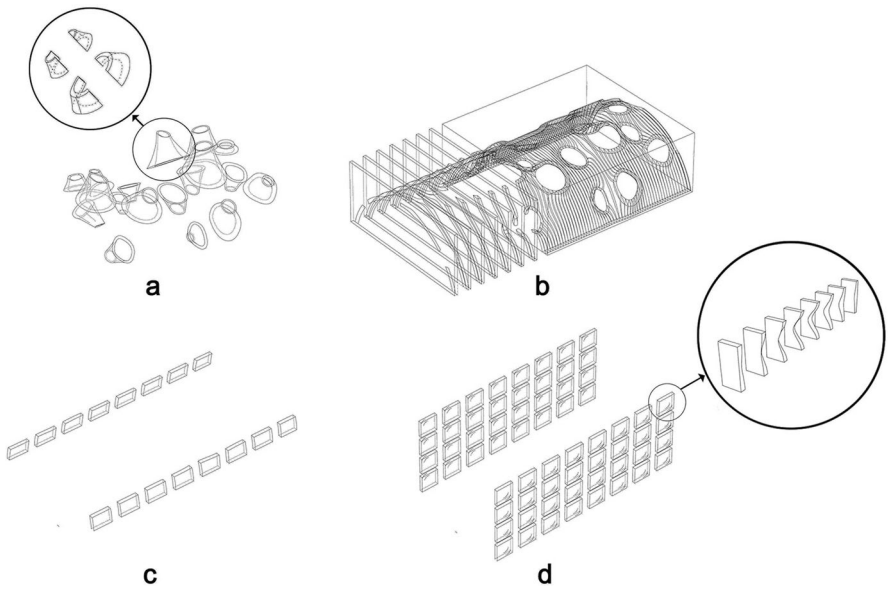


Fig. 11 Four sections dissected for hot-wire cutting

### Fabricating Components

In addition to generating new design possibilities, the capability to fabricate a physical assembly is crucial for the effective design completion. Detailed data regarding prototype cutting are hierarchically documented on a computer. First, fabrication accuracy is essential to ensure the quality and integrity of the output. As mentioned earlier, calibration of the hot-wire cutter is crucial for ensuring

the accuracy of each component. The relationship between the feed rate and heat strength must be examined to reduce errors and deviations. Certain unfavorable phenomena occur in practical cutting scenarios, such as the curving of a straight wire (called the bowing effect) or motor-induced vibration of the wire (Park et al. 2021). Occasionally, the hot wire loosens or servers when the feed rate and heat intensity are inappropriate. This also causes the cut surface to become rough or severely rippled. The tolerance and accuracy of the components are affected by various cutting scenarios and setting conditions. The object is then trimmed by controlling the robot pad. The wire cutter moves in a perpendicular direction to the surface such that the toolpaths are smoothly controlled. An appropriate feed rate and heat would enable smooth and consistent cutting. A few test cuttings are executed to obtain the optimal surfaces and shapes and to examine whether errors or discrepancies exist between the simulated and trimmed outputs. Inaccurate cutting causes problems during the assembly. In addition, the original design requires occasional and minor alterations to accommodate the fabrication difficulties.

In our experiment, pieces were cut sequentially. Among the four sections of the model, sections C and D were straightforward to cut. However, in section A, the cone shapes had different thicknesses and forms. Therefore, they were cut off with special precautions. All the components were cut using one or two cutter movements. In section B, the robot's movement path was set and operated several times to recut the parts owing to the greater radius of curvature inside and outside the conical shapes. Certain pieces were meticulously cut owing to the complexity of their geometries (Fig. 12).

The cutting process is typically time-consuming. Furthermore, marginal mistakes or negligence yield components incompatible with other parts. Accordingly, the test assembly process was performed simultaneously with fabrication in our research laboratory. This was performed to examine whether the components fit each other appropriately (Fig. 13). Some discrepancies and errors were observed between the different components during preassembly. However, this process was essential for identifying marginal cutting errors, ensuring the correctness of the sizes and shapes of each component, appropriate combinations of components, and sequencing of fabrication activities. When incorrect pieces were identified, they were placed on the spot. However, the retrimming during this process is problematic. Certain parts of the unit components must be marginally adjusted or retrimmed. The sizes and shapes of the pre-assembled components were determined using 3D drawings. Therefore, errors were identified and corrected before components were glued together.

## Assembly and Installation

After cutting all the components, they were laid out, sequentially assembled, and installed in place (Fig. 14). Based on the numbered templates, each component was accurately fixed at its position. The size and shape of each component had to be accurate because the positions of the unit components were relative to each other (Park 2013). A single misalignment could cause deformation of the entire structure and would yield an ineffective fabrication result.

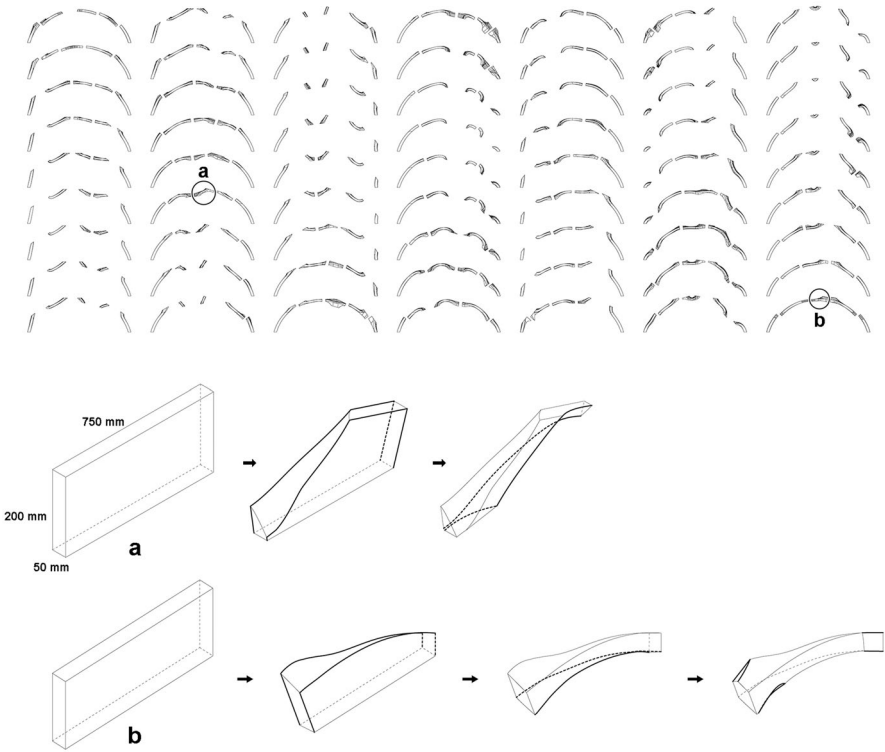


Fig. 12 63 pieces of section B (top) and two examples depicting different phases of cutting the pieces (bottom)

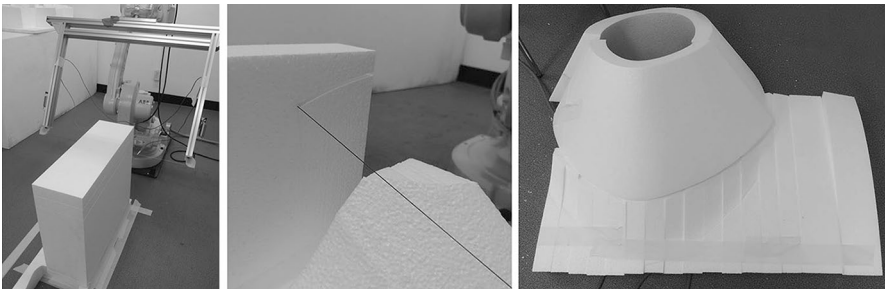


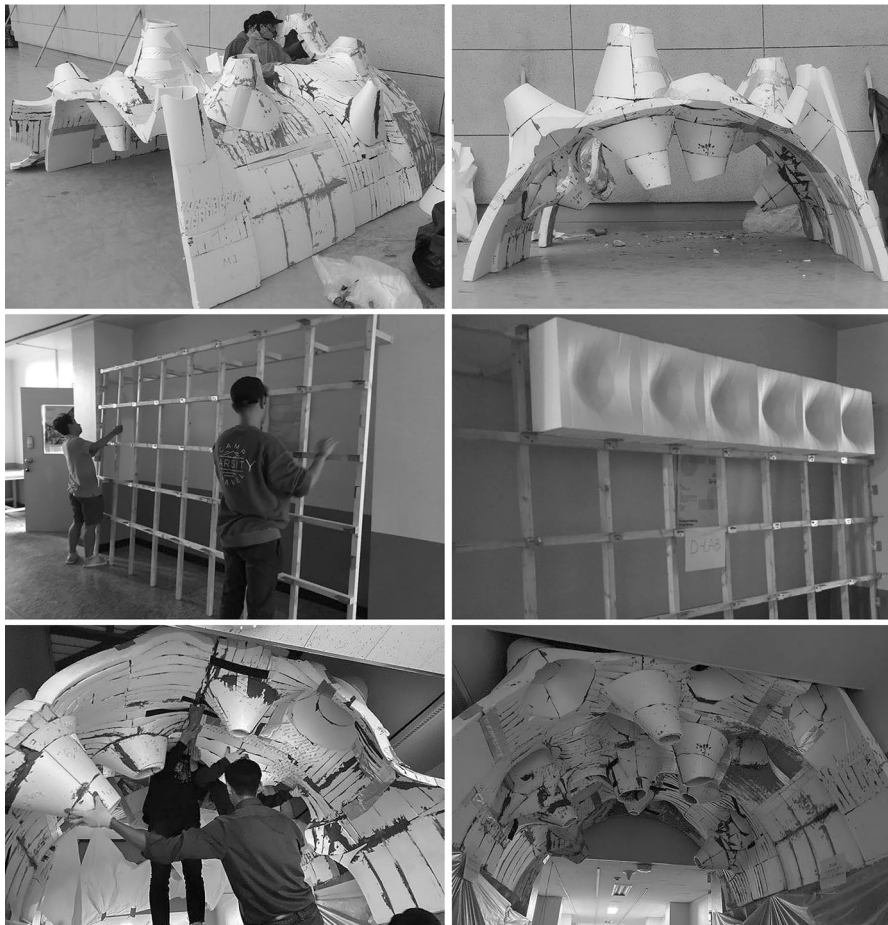
Fig. 13 The cutting test and the preassembly adjustment

We thought that it was difficult for the whole roof to pre-assemble at once onsite and lift it to the roof position because of its weight and the size of the corridor. We decided that the whole structure should be divided into two basic parts, wall, and roof, and then assembled in order. For the wall, the wooden frame was installed and fixed to safely support the wall pieces, and then the components were positioned in



place, one by one. Anchor bolts affixed the frame to the wall, and a metal bracket was used to safely install each component. The roof was carefully divided into five parts ranging from 400 to 700 mm in width. Each part was lifted and fixed.

The assemblies of various adhesives were tested. First, an acrylic Styrofoam bond mixed with a mortar was used to determine the degree of coupling between the components. However, the strength and elasticity of this adhesive are low for a large structure; hence, the adhesive surface occasionally splits or falls. Next, a Styrofoam bond resin was applied, because a marginal amount of this adhesive is known to secure a high bond strength. The final assembled design hardened after several days. The model was sanded along common joining faces until it became marginally finer. Finally, the edges and surfaces of the assembled components were sanded and finished using thin cementitious polymer mortar. This resulted in a smooth surface.



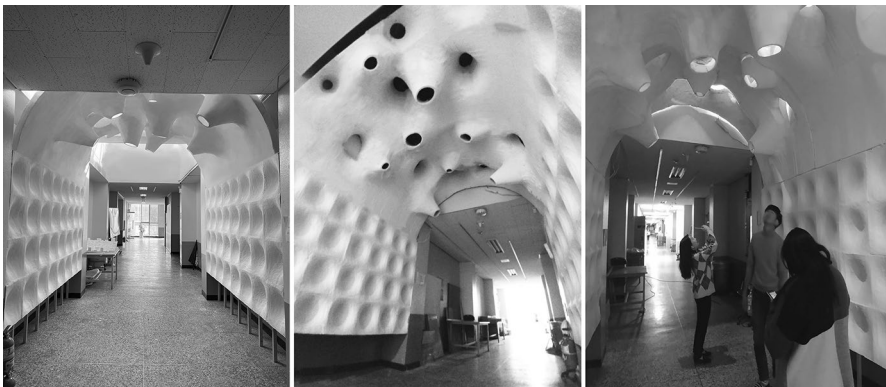
**Fig. 14** Completion of the partial assembly of components; installation of the assembled components on-site

When the assembly was completed, the installation was kept in place for three weeks and then dismantled (Fig. 15). Note that the structure is a custom-made design in which each component has a different shape and size. Moreover, the assembly of components is similar to the artisan process of combining components. This design is difficult to implement in ordinary construction. The project functions as a testbed for the interactive collaboration between innovative design concepts and construction solutions. The results of the design implementation, structural conditions, and spatial effects of natural light infiltration through the shell dome are considered effective. As anticipated, this structure has become a focal point for striking dynamism among users.

## Conclusion

This study addressed the key issues underlying the collaborative efforts between form-finding and robotic fabrication integrated with technical support. Such efforts are considered complementary processes in design realization. Form-finding using the circle packing method allows for the generation of variable parametric shell designs by simply altering or specifying certain parameters of a primitive shell design, much beyond the traditional shell structure. Notably, designs can be readily created through various form-finding processes using digital tools. These processes generate unique parametric shell designs that also form a new design language. With the help of current technologies, it is possible to generate variable designs, analyze them structurally, and fabricate them accurately, efficiently, and cost-effectively.

A critical phase in this process is the transformation of a digital model that uses precise data with a set of components for the fabrication and assembly of the model. The data of the parametric design transfers to a separate fabrication. This approach has rarely been integrated within the present architectural practice. One of the major challenges in this collaboration is that architects need software scripting and hardware knowledge for the development of custom-made end-effectors and



**Fig. 15** Final images captured during the day and night (left and middle), and an image that shows how people interact with the project (right)

tools for robots. This is because end-effectors (e.g., hot wire, grappler, and drill) are custom-made and tailored to satisfy specific requirements and for specific tasks. Further tests and design explorations with other end-effectors will be carried out to develop tools other than the simple hot-wire cutter.

To sum up, this study suggests that the interactive process is an effective method in the production of free-form structures. This hotwire cutting method shows that an increasing accuracy can be achieved for curved cuts. Despite the significant advantages and potential of this process, some deficiencies still need to be addressed. It is undeniable that the fabrication process results in the wastage of materials. In the future, the accuracy of the cutting method should be improved and new approaches to produce different forms should be further examined. The assembly process was not as smooth as expected and was labor-intensive. Furthermore, fatigue for accurate assembly was still high. Nevertheless, technological advancements that allow for the computer-aided development of designs challenge architects and the way they usually work. The entire procedure proves to be a valuable experiment for further implementation of form-making and fabrication in the design of full-scale architectural designs.

**Acknowledgements** This study was supported by the Basic Science Research Program through the National Research Foundation of Korea (NRF) funded by the Ministry of Education (NRF-2021R1A2C1093869). All figures are by the authors.

## References

- Aitchison, David, Brooks Hadley, Bain Joseph and Pons Dirk. 2011. Rapid manufacturing facilitation through optimal machining prediction of polystyrene foam. *Virtual and Physical Prototyping* 6(1): 41–46.
- Bechtold, Martin. 2008. *Innovative Surface Structures, Technologies and Applications*. Taylor & Francis.
- Duenser, Simon, Poranne Roi, Thomaszewski Bernhard and Coros Stelian. 2020. Robot Cut: Hot-wire Cutting with Robot-controlled Flexible Rods. *ACM Transaction on Graphics* 39(4): 98:1–15.
- Hawkins, Will, Herrmann, Michael, Ibell, Tim, Kromoser, Benjamin, Michaelski, Alexander, Orr, John, Pedreschi, Remo, Pronk, Aron, Schipper, Roel, Shepherd, Paul, Veenendaal, Diederik, Rene Wansdronk and Mark West. 2016. Flexible formwork technologies: a state of the art review. *Structural Concrete* 17(6): 911–935.
- Jovanovic, Marko, Vucic, Marko, Mitov, Dejan, Tepavčević, Bojan, Vesna Stojakovic and Ivana Bajanski. 2017. Case specific robotic fabrication of foam shell structures. *Proceedings of the 35th International Conference on Education and Research in Computer Aided Architectural Design in Europe (eCAADe)* 2: 135–142.
- Meryem Yabanigül and Turgul Yazar. 2021. Production of Gyroid-like modular systems with non-linear robotic hotwire cutting. *Automation in Construction*. 126: 1–18.
- Park, Seungbeom, Park, Jin-Ho, Sejung Jung and Su-Jung Ji. 2021. Foam Cutting for an Architectural Installation using Industrial Robot Arm: Calibration, Error, and Deviation Analysis. *Automation in Construction* (133):1–10.
- Park, Jin-Ho. 2013. *Graft in Architecture: Recreating Spaces*. Images Publishing.
- Reinhardt, Dagmar, Rob Saunders and Jane Burry. 2016. eds, *Robotic Fabrication in Architecture, Art and Design 2016*. Springer.
- Rust, Romana, Jenny, David, Fabio Gramazio and Matthias Kohler. 2016. Spatial wire cutting: Cooperative robotic cutting of non-ruled surface geometries for bespoke building components. CAADRIA 2016, 21st International Conference on Computer-Aided Architectural Design Research in Asia-Living Systems and Micro-Utopias: Towards Continuous Designing, Melbourne, Australia.

- Sharif, Shani, Russell Gentry and Larry Sweet. 2016. Human-Robot Collaboration for Creative and Integrated Design and Fabrication Processes. 2016 Proceedings of the 33rd ISARC (The International Association for Automation and Robotics in Construction), Auburn, USA, 596–604.
- Symeonidou, Ioanna, Urs Leonhard Hirschberg and Martin Kaftan. 2013. Designing the Negative. In *Computation and Performance* (Vol.1: 683–691). Proceedings of the 31st eCAADe Conference. eCAADe and Faculty of Architecture TU Delft.
- Wes McGee and Monica Ponce de Leon. 2014. eds, *Robotic Fabrication in Architecture, Art and Design 2014*. Springer.
- Weissenböck, Renate. 2015. Robotic Design-Fabrication: Exploring Robotic Fabrication as a Dynamic Design Process. Proceedings of the 33rd eCAADe Conference, Vienna, Austria, 309–318.
- Willmann, Jan, Block, Philippe, Hutter, Macro, Kendra Byrne and Tim Schork. 2018. eds, *Robotic Fabrication in Architecture, Art and Design 2018*, Springer.

**Publisher's Note** Springer Nature remains neutral with regard to jurisdictional claims in published maps and institutional affiliations.

Springer Nature or its licensor (e.g. a society or other partner) holds exclusive rights to this article under a publishing agreement with the author(s) or other rightsholder(s); author self-archiving of the accepted manuscript version of this article is solely governed by the terms of such publishing agreement and applicable law.

**Jin-Ho Park** teaches architectural design, theory, and history as a professor in the Department of Architecture at Inha University, Korea. Prior to joining Inha University, he taught in the School of Architecture at the University of Hawaii at Manoa, USA as an associate professor with tenure. He earned his Ph.D. in architecture from University of California, Los Angeles (UCLA). His book publications include *Architectural and Urban Subsymmetries* (Birkhauser,2022), *Graft in Architecture: Recreating Spaces* (Images Publishing, 2013) and *Designing the Ecocityin-the-Sky* (Images Publishing, 2014).

**Sejung Jung** is a Ph.D candidate in the Department of Architecture at Inha University.